Inorganic Chemistry

ARTICLE

pubs.acs.org/IC

Influence of Electron Delocalization in Heterocyclic Core Systems on the Electrochemical Communication in 2,5-Di- and 2,3,4,5-Tetraferrocenyl Thiophenes, Furans, and Pyrroles

Alexander Hildebrandt, Dieter Schaarschmidt, Ron Claus, and Heinrich Lang*

Department of Chemistry, Chair Inorganic Chemistry, Chemnitz University of Technology, Strasse der Nationen 62, 09111 Chemnitz, Germany

Supporting Information

ABSTRACT: A series of 2,5-di- and 2,3,4,5-tetraferrocenyl-substituted thiophenes, furans, and pyrroles were synthesized using the Negishi *C,C* cross-coupling protocol. The electronic and electrochemical properties of these compounds were investigated by cyclic voltammetry (CV), square wave voltammetry (SWV), and in situ UV−vis/NIR spectroscopy. The molecular structures of 2,5-diferrocenyl furan and 2,3,4,5-tetraferrocenyl-1-methyl-1*H*-pyrrole in the solid state are discussed. The ferrocenyls could sequentially be oxidized giving two or four reversible responses for the appropriate di- or tetraferrocenyl-substituted heterocyclic molecules. The observed $\Delta E^{o\prime}$ values range between 186 and 450 mV. The NIR measurements confirm electronic communication as intervalence charge transfer (IVCT) absorptions were found in the corresponding mono- and in case of the tetraferrocenyl compounds also in the dicationic species. All compounds, except tetraferrocenyl thiophene (a class I system), were classified as class II systems according to Robin and Day. They show a linear relationship between $\Delta E^{o\prime}$ and the IVCT oscillator strength *f* which could be shown for the first time in organometallic chemistry. This was possible because the series of molecules exhibit analogous geometries and hence, similar electrostatic properties. This correlation was confirmed by electro- and spectro-electrochemical measurements. Within these studies a new approach for the estimation of the effective electron transfer distances r_{ab} is discussed.

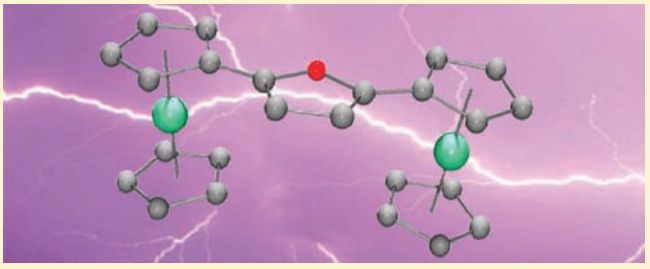

INTRODUCTION

Electronic communication of mixed-valent species in organometallic,[1] metal−organic,[2] or organic compounds[3] has drawn increasing interest during recent years because they can be used as model systems to study electron transfer through π-conjugated carbon-rich organic linking units and hence, may be used for the design of novel electro-active materials.[4] Especially organometallics such as ferrocenes, ruthenocenes, and iron or ruthenium halfsandwich compounds have been frequently used as redox-active functionalities.[1,5] The degree of communication among the metal centers through the π-conjugated bridge has mostly been investigated by electrochemical studies including cyclic voltammetry (CV), square wave voltammetry (SWV), as well as spectroelectrochemistry (e.g., in situ UV−vis/NIR, IR spectroscopy).[6]

Modification of the π-conjugated connectivities allows the examination of the influence on the intermetallic communication, whereby the redox-splitting depends on the connectivity length as it could be shown, for example, in ferrocenyl- or Fe(η^5-C_5H_5)(η^2-dppe)-substituted ethynes, buta-1,3-diynes, or even more extended carbon chains.[7] Furthermore, the influence of different substitution patterns in aromatics on their electrochemical behavior has been studied, for instance on di-, tri-, and tetraferrocenyl functionalized benzenes.[8]

The aforementioned organometallic species differ in their geometries resulting in a change of the electrostatic contribution to the splitting of their redox potentials. Therefore, the electrochemical data of these molecules do not allow easy comparison with one another. This prompted us to synthesize a series of 2,5-di- and 2,3,4,5-tetraferrocenyl thiophenes, furans, and pyrroles as the electrostatic contribution to the separation of the half wave potentials ($\Delta E^{o\prime}$) should be very similar. Hence, $\Delta E^{o\prime}$ should directly correspond to the appropriate communication properties. This would additionally allow to investigate the influence of electron delocalization on the electrochemical communication in the appropriate heterocyclic species. On the basis of our recent electrochemical studies on ferrocenyl-substituted heterocycles,[9−11] we here report for the first time on the synthesis and electrochemical behavior of a series of 2,5-di- and 2,3,4,5-tetraferrocenyl-substituted heterocyclic compounds.

RESULTS AND DISCUSSION

Synthesis and Characterization. The 2,5-di- and 2,3,4,5-tetraferrocenyl-substituted heterocycles **3a**−**d** and **5a**−**d**,

Received: May 3, 2011
Published: September 29, 2011

Scheme 1. Synthesis of 3a−d from 1a−d and 5a−d from 4a−d and 2[a]

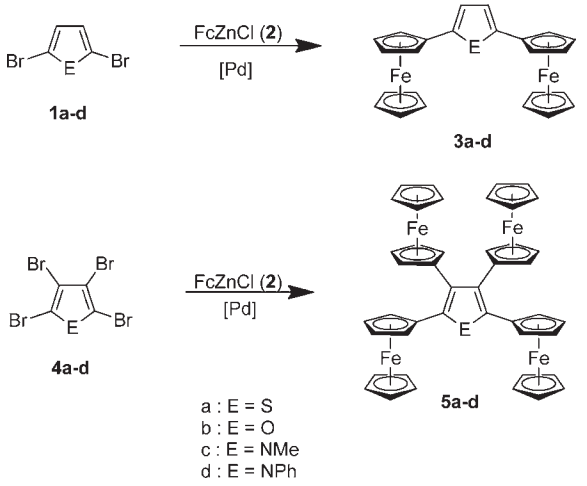

[a] [Pd] = $Pd(PPh_3)_4$ tetrahydrofuran, 60 °C, 48 h; Fc = $Fe(\eta^5\text{-}C_5H_5)(\eta^5\text{-}C_5H_4)$.

respectively, were accessible by Negishi ferrocenylation of the appropriate bromo-substituted derivatives **1a−d** or **4a−d** with FcZnCl (**2**) (Fc = $Fe(\eta^5\text{-}C_5H_5)(\eta^5\text{-}C_5H_4)$), accessible by monolithiation of ferrocene according to Sanders and Mueller-Westerhoff[12] followed by treatment with dry zinc chloride, in presence of catalytic amounts of tetrakis(triphenylphosphane)-palladium(0) (Scheme 1). The dibromo species **1a−d** were prepared by reacting the appropriate heterocycles with 2 equiv of *N*-bromosuccinimide, while the respective tetrabromo derivatives **4a−d** were available under varying reaction conditions. Compound **4a** was prepared by treatment of thiophene with bromine in the presence of iron turnings.[13] In contrast to this, molecules **4c** and **4d** were obtained by a 4-fold bromation of the appropriate pyrrole as described for **1a−d**,[14] while **4b** had to be synthesized by a 2-fold dehydrobromination of hexabromotetrahydrofuran according to Hill and Sanger.[15]

Organometallics **3a−d** and **5a−d** are stable in air and moisture both in the solid state and in solution. They have been identified by elemental analysis as well as IR, UV−vis, and NMR (^1H, $^{13}C\{^1H\}$) spectroscopies. High resolution-ESI TOF mass-spectrometry and single crystal X-ray structure analysis (**3b** and **5c**) were additionally carried out. The electrochemical behavior of all compounds (cyclic voltammetry (CV), square wave voltammetry (SWV); UV−vis/NIR spectroscopy between 280−3000 nm) was determined as well.

In the ^1H NMR spectra of the 2,5-diferrocenyl compounds **3a−d** one characteristic resonance signal for the aromatic core protons at 6.81 (**3a**), 6.21 (**3b**), 6.23 (**3c**), or 6.33 ppm (**3d**) is observed. For the ferrocenyl units one singlet (C_5H_5) and two pseudotriplets with J_{HH} = 1.8 Hz (C_5H_4) as it is typical for AA′XX′ spin systems have been found (Experimental Section, Supporting Information, Figures SI6−SI9, and refs 9,11). The steric demand of the ferrocenyl substituents in supercrowded **5a−d** causes an increase of the signal broadness of the C_5H_4 protons. This behavior is mostly pronounced in phenylpyrrole **5d** caused by the additional steric demand of the phenyl group. Conspicuous is that the resonance signal of the CH_3 protons in **5c** is significantly shifted to lower field (4.76 ppm), when compared with **3c** (3.78 ppm).

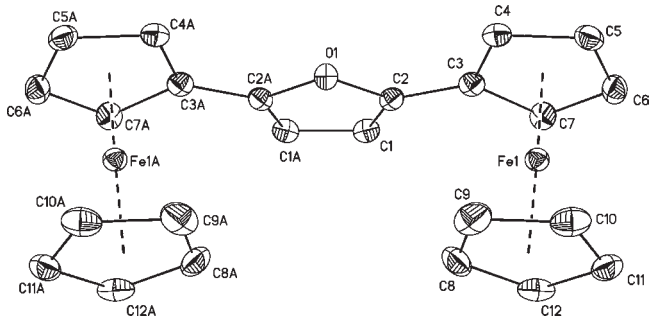

Figure 1. ORTEP diagram (50% probability level) of the molecular structure of **3b** crystallized from a choloroform/*n*-hexane mixture, with the atom-numbering scheme. All hydrogen atoms have been omitted for clarity. Selected bond distances (Å), angles (deg), and torsion angles (deg): D1−Fe1 1.6462(2), D2−Fe1 1.6434(2), O1−C2 1.3766(15), C1−C2 1.3541(19), C1−C1A 1.421(3), C2−C3 1.4456(19), C1−C2−O1 109.76(12), C2−O1−C2A 106.68(14), C1−C2−C3 133.34(13), D1−Fe1−D2 178.47(2), C1−C2−C3−C4 171.41(14), C1A−C1−C2−O1 −0.61(12) (D1 denotes the centroid of C_5H_5 at Fe1; D2 denotes the centroid of C_5H_4 at Fe1). (Symmetry generated atoms are indicated by the suffix A; symmetry code: *x*, −*y*+1/2, *z*.).

Single crystals of **3b** and **5c** suitable for X-ray diffraction analysis could be obtained by diffusion of *n*-hexane into a chloroform solution containing **3b** or **5c** at ambient temperature. The molecular structure of **3b** in the solid state is shown in Figure 1, and the one of **5c** in Figure 2. Important bond distances (Å), bond angles (deg), and torsion angles (deg) are summarized in the caption of Figure 1 (**3b**) or Figure 2 (**5c**). For crystal and structure refinement data see Experimental Section.

2,5-Diferrocenyl furan **3b** crystallized in the orthorhombic space group *Pnma* as orange needles. In contrast to 2,5-diferrocenylthiadiazole[10] the ferrocenyl substituents are oriented to the same side. They are rotated by 11.30 (5) ° out of the plane of the furan core. The cyclopentadienyl ligands at the iron centers show an almost staggered conformation (−5.3(1)°). As expected, the $^cC_4H_2O$ core is planar (r. m. s. deviation 0.0039 Å, highest deviation from planarity observed for O1 with −0.0054(10) Å).

In crystals of 2,3,4,5-tetraferrocenyl-1-methyl-1*H*-pyrrole **5c** the molecules are packed in the orthorhombic space group *Aba*2. As is common for hetero aromatic compounds the ^cC_4N arrangement is planar (r. m. s. deviation 0.0177 Å, highest deviation from planarity observed for C2 with −0.0247(22) Å). The cyclopentadienyls at the iron atoms exhibit an almost staggered conformation (−7.7(3) for Fe1, −1.5(3) for Fe2, −1.7(3) for Fe3, and 4.3(3)° for Fe4, respectively). The ferrocenyl ligands are rotated by 46.45(13) (Fe1), 48.43(13) (Fe2), 47.15(13) (Fe3), and 37.82(14)° (Fe4) out of the plane of the pyrrole core.

To achieve a high degree of intermetallic electron transfer interaction the π-systems of both the ferrocenyls' cyclopentadienyls and the heterocyclic core have to be coplanar. The torsion of the substituents in the solid state found in **5c** would argue for weak interactions. However, corresponding *N*-phenyl pyrrole **5d** which exhibits a hindered rotation of the ferrocenyl substituents in solution at room temperature (2,5-position: $\Delta H^{\ddagger}$ = 26.8 (±1.2) kJ·mol^{-1}, $\Delta S^{\ddagger}$ = −94.1 (±4.5) J·mol^{-1}·K^{-1}; 3,4-position: $\Delta H^{\ddagger}$ = 27.9 (±1.5) kJ·mol^{-1}, $\Delta S^{\ddagger}$ = −88.6 (±5.6) J·mol^{-1}·K^{-1}) shows strong electronic communication.[11] Such rotation barriers in solution were not determinable by VT-NMR for compounds **5a−c**. On the basis of these observations, the

dx.doi.org/10.1021/ic200926z |*Inorg. Chem.* 2011, 50, 10623–10632

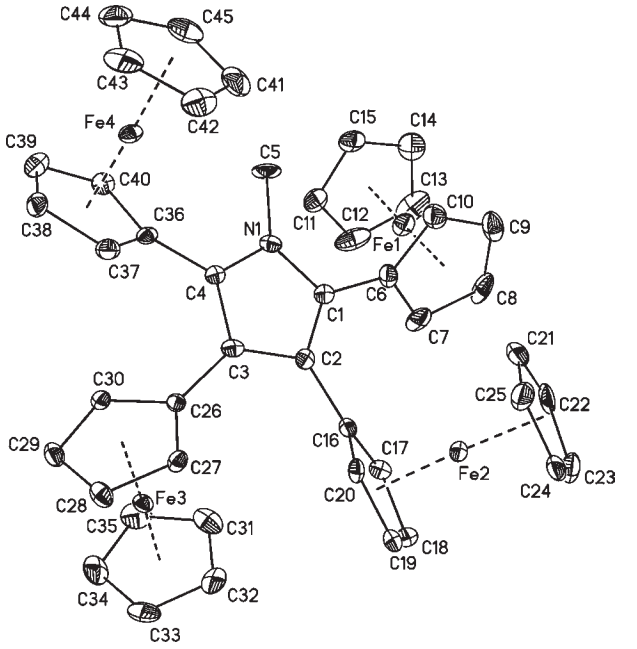

Figure 2. ORTEP diagram (50% probability level) of the molecular structure of **5c** crystallized from a choloroform/*n*-hexane mixture, with the atom-numbering scheme. All hydrogen atoms and two molecules of chloroform have been omitted for clarity. Selected bond distances (Å), angles (deg) and torsion angles (deg): D1−Fe1 1.6659(5), D2−Fe1 1.6612(5), D3−Fe2 1.6515(5), D4−Fe2 1.6545(5), D5−Fe3 1.6486(5), D6−Fe3 1.6491(5), D7−Fe4 1.6559(5), D8−Fe4 1.6482(5), C1−C2 1.391(5), C2−C3 1.442(5), C3−C4 1.381(4), N1−C1 1.387(4), N1−C4 1.362(4), N1−C5 1.473(4), C1−C6 1.465(5), C2−C16 1.484(5), C3−C26 1.483(5), C4−C36 1.472(5); N1−C1−C2 107.8(3), C1−C2−C3 106.6(3), C1−N1−C4 109.5(3), C1−N1−C5 126.9(3), D1−Fe1−D2 177.11(4), D3−Fe2−D4 176.24(4), D5−Fe3−D6 177.45(4), D7−Fe4−D8 175.49(4); N1−C1−C2−C3 4.2(4), C6−C1−C2−C16 2.7(7), N1−C1−C6−C10 47.6(5), N1−C4−C36−C37 −142.1(4), C1−C2−C16−C20 131.7(4), C4−C3−C26−C27 −131.8(4) (D1, D3, D5, D7 denote the centroids of C_5H_4 at Fe1−Fe4; D2, D4, D6, D8 denote the centroids of C_5H_5 at Fe1−Fe4).

impact of the steric hindrance on the electron transfer properties seems to be negligible.

Electron delocalization in heterocyclic **3a**−**d** and **5a**−**d** can be expressed by comparison of the formal C=C double bonds (for example, C1−C2 (1.391(5) Å), C3−C4 (1.381(4) Å) in **5c**) and the inner carbon−carbon single bond (for **5c** C2−C3 (1.442(5) Å), Figure 2). For aromatics double bonds are longer than isolated double bonds ($d^0_{C=C}$ = 1.34 Å[16]) and single bonds are shortened compared to isolated *C,C* single bond distances (d^0_{C-C} = 1.54 Å[16]). To compare the delocalization among different aromatic molecules (see above) the parameter τ as normalized quotient of the single and double bond lengths is introduced (eq 1). Completely delocalized systems such as benzene evince a τ value of 1, while for localized systems τ approaches 0

$$\tau = 1 + \frac{(d_{C-C}/d_{C=C}) - 1}{1 - (d^0_{C-C}/d^0_{C=C})} \qquad (1)$$

where d_{C-C} = 1.54 Å, $d_{C=C}$ = 1.34 Å, d_{C-C} = distance of the appropriate single bond, $d_{C=C}$ distance of the appropriate double bond.

Table 1. Bond Distances and Delocalization Parameters τ of 3b, 5a, 5c, and 5d

compound	d_{C-C} (Å)	$d_{C=C}$ (Å)	τ	ref.
3b	1.421(3)	1.3541(19)	0.669	this work
5a	1.493(13)	1.370(13)	0.398	9
5c	1.442(5)	1.391(5)	0.754	this work
5d	1.435(3)	1.400(3)	0.832	11

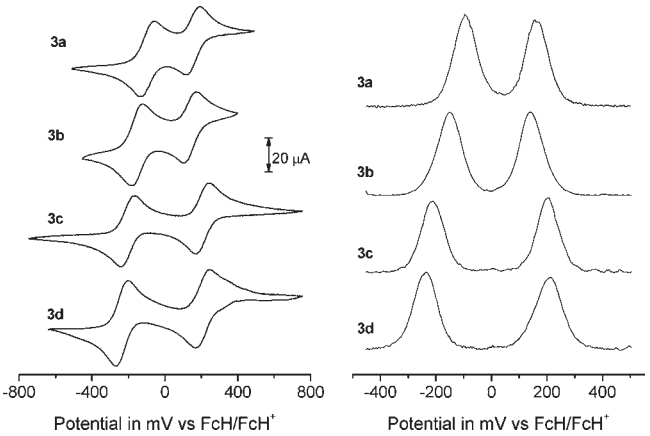

Figure 3. Left: Cyclic voltammograms of **3a**−**d**; scan rate: 100 mV. Right: Square wave voltammograms of **3a**−**d** in dichloromethane solutions (1.0 mmol·L^{-1}) at 25 °C, supporting electrolyte [N^{n}Bu$_4$][B(C$_6$F$_5$)$_4$] (0.1 mol·L^{-1}). For $\Delta E^{o\prime}$ values see Table 2.

The τ parameters for heterocycles **3b**, **5a**, **5c**, and **5d** are summarized in Table 1 revealing that the electrons in the thiophene core of **5a** are less delocalized when compared to pyrroles **5c** and **5d**, which most probably is attributed to the different heteroatoms present in the five-membered rings. The electrons of the ferrocenyl substituted heterocycles are less delocalized than in unsubstituted pyrrole (τ = 0.830), thiophene (τ = 0.741), and furan (τ = 0.660),[17] respectively. While pyrroles **5c** and **5d** as well as furan **3b** exhibit τ values close to those of the appropriate unsubstituted heterocycles, 2,3,4,5-tetraferrocenyl thiophene **5a** shows with τ = 0.398 a significant smaller value. This indicates that the electrons in the ^{c}C$_4$S core of **5a** are substantially more localized than in thiophene itself. Information derived from this parameter should be treated with caution because not only the electronic properties contribute to the appropriate bond lengths but also steric hindrance. Nevertheless hints on the possible intermetallic communication can be derived from the τ values.

Despite the significantly longer carbon element distances in thiophene **5a** (1.731(11); 1.704(9) Å) in comparison with pyrroles **5c**,**d** (1.381(4), 1.387(4) Å **5c**; 1.393(3), 1.394(3) Å **5d**), or furan **3b** (1.3766(15) Å), the distances between the *ipso*-carbons of the respective ferrocenyl units are only slightly affected (maximum deviation <5%). (Supporting Information, Table SI1) Therefore, the electron transfer distances in this series are almost equal which should result in similar electrostatic interactions.

Electro- and Spectro-Electrochemistry. The redox properties of **3a**−**d** and **5a**−**d** were studied by cyclic voltammetry (CV), square wave voltammetry (SWV) (see Figure 3 and Figure 8), and UV−vis/NIR spectroscopy (Figures 4 and 9).

dx.doi.org/10.1021/ic200926z |*Inorg. Chem.* 2011, 50, 10623–10632

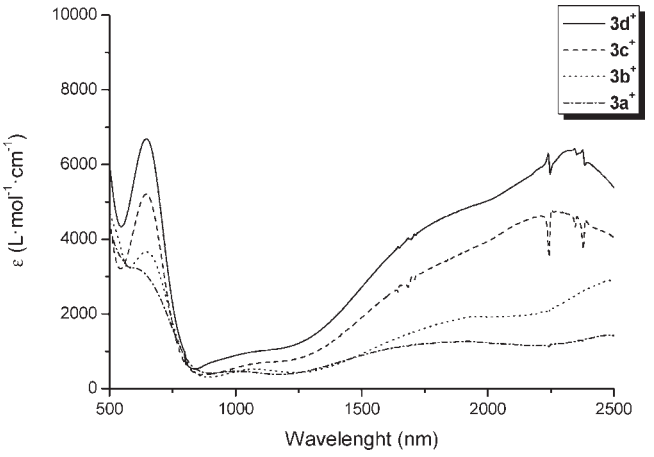

Figure 4. UV-vis/NIR spectra of in situ generated $\mathbf{3a}^+-\mathbf{3d}^+$ at 25 °C in dichloromethane (c = 1.0 mmol·L^{-1}); supporting electrolyte [N^{n}Bu$_4$][B(C$_6$F$_5$)$_4$] (0.1 mol·L^{-1}).

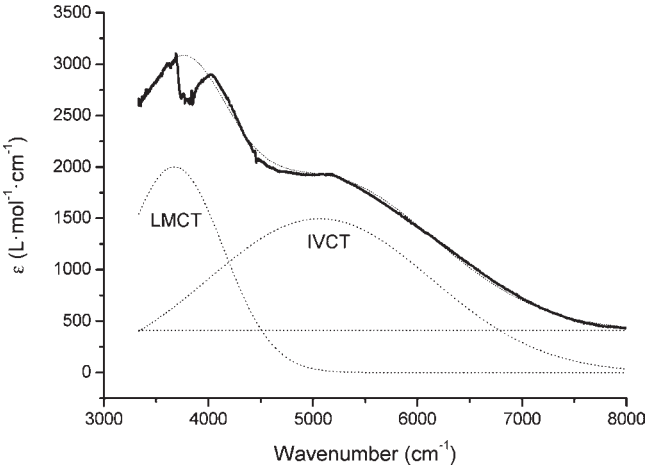

Figure 6. Deconvolution of the NIR absorptions of $\mathbf{3b}^+$ using three Gaussian shaped bands determined by spectro-electrochemistry in an OTTLE cell.

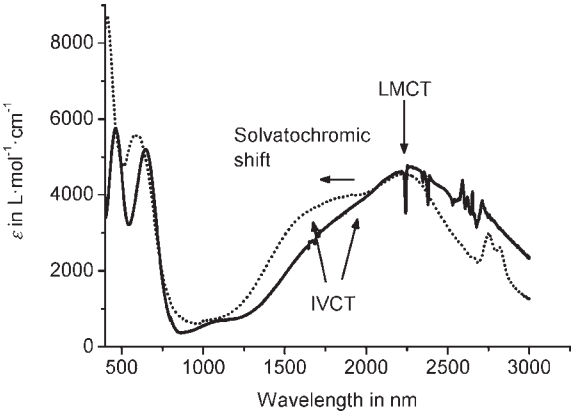

Figure 5. Solvatochromic behavior of the NIR spectra of $\mathbf{3c}^+$ (1.0 mmol·L^{-1}) at 25 °C, supporting electrolyte [N^{n}Bu$_4$][B(C$_6$F$_5$)$_4$] (0.1 mol·L^{-1}); solid, dichloromethane; dotted, acetonitrile.

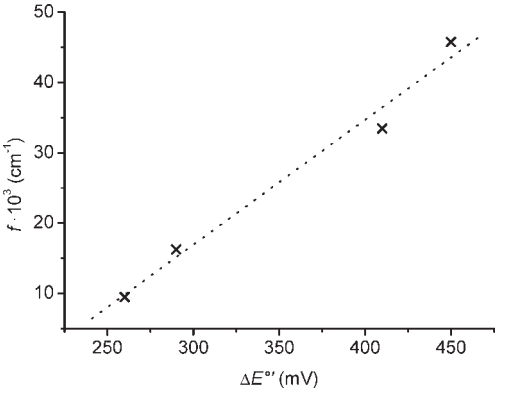

Figure 7. Correlation of the oscillator strength f of the IVCT absorptions and the $\Delta E^{\circ\prime}$ values of **3a**−**d** determined by NIR and cyclic voltammetry, respectively.

Dichloromethane solutions of [N^{n}Bu$_4$][B(C$_6$F$_5$)$_4$] (c = 0.1 mol·L^{-1}) were used as supporting electrolyte.[18] The cyclic voltammetric studies were carried out at a scan rate of 100 mV·s^{-1} and are summarized in Tables 2 (**3a**−**d**) and 3 (**5a**−**d**). All potentials were referenced to the FcH/FcH$^+$ redox couple.[19] The redox processes occur between −240 to 215 mV for **3a**−**d** and −280 to 610 mV for **5a**−**d**.

Figure 3 shows the cyclic and square wave voltammograms of the 2,5-diferrocenyl heterocycles **3a**−**d** with two individual reversible events (CV: ΔE_p values of 60 to 75 mV). Thiophene **3a** exhibits with −94 mV the highest potential for its first oxidation. All other compounds are easier to oxidize (−152 mV (**3b**), −206 mV (**3c**), −238 mV (**3d**)) and hence are more electron-rich (Table 2). Moreover, the $\Delta E^{\circ\prime}$ values increase from **3a** (260 mV) over **3b** (290 mV) and **3c** (410 mV) to **3d** (450 mV) indicating that the more electron-rich systems within this series exhibit higher $\Delta E^{\circ\prime}$ values, and, hence, a higher degree of intermetallic communication is expected (see below).

The spectro-electrochemical studies were performed by stepwise increase of the potential from −500 to 1200 mV vs Ag/Ag$^+$ in an OTTLE cell (OTTLE = Optically Transparent Thin-Layer Electrolysis) containing dichloromethane solutions of **3a**−**d** (1.0 mmol·L^{-1}) and [N^{n}Bu$_4$][B(C$_6$F$_5$)$_4$] (0.1 mol·L^{-1}) as electrolyte. The potential increase was performed using varying step heights of 25 mV, 50 mV, and 100 mV, respectively. During this procedure **3a**−**d** were oxidized to the mixed-valent 2,5-diferrocenyl species $\mathbf{3a}-\mathbf{d}^+$ and finally to dicationic $\mathbf{3a}-\mathbf{d}^{2+}$. UV−vis/NIR spectra of the neutral 2,5-diferrocenyl heterocycles **3a**−**d** show exclusively ferrocenyl-based d-d absorptions at 455 nm. As the potentials rise to 200−350 mV vs Ag/Ag$^+$ (**3a**, 350 mV; **3b**, 300 mV; **3c**, 250 mV; **3d**, 200 mV) oxidation takes place, whereby the mixed-valent species $\mathbf{3a}-\mathbf{d}^+$ were formed. This is supported by the observation of intervalence charge transfer (IVCT) absorptions with varying extinctions as well as ligand-to-metal charge transfer (LMCT) transitions at about 650 nm (Figure 4). Upon further potential increase to 600 and finally to 1200 mV dicationic $\mathbf{3a}-\mathbf{d}^{2+}$ were generated. As expected, the IVCT absorptions disappear during this second oxidation process and can be observed in the spectral range between 850 and 1000 nm absorptions. Those bands can be assigned to LMCT absorptions because of characteristic ν and $\Delta\nu_{1/2}$ values (Table 4 and Supporting Information, Figures SI1−SI3). The assignment

dx.doi.org/10.1021/ic200926z |Inorg. Chem. 2011, 50, 10623–10632

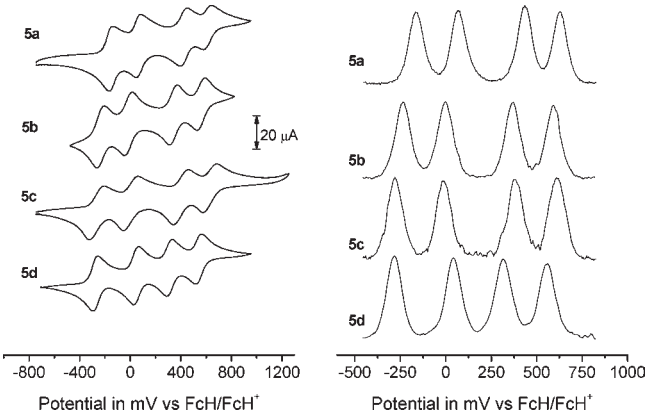

Figure 8. Left: Cyclic voltammograms of **5a**−**d**; scan rate: 100 mV. Right: Square wave voltammograms of **5a**−**d** in dichloromethane solutions (1.0 mmol·L^{-1}) at 25 °C, supporting electrolyte [N^{n}Bu$_4$][B(C$_6$F$_5$)$_4$] (0.1 mol·L^{-1}). For $\Delta E^{o\prime}$ values see Table 3.

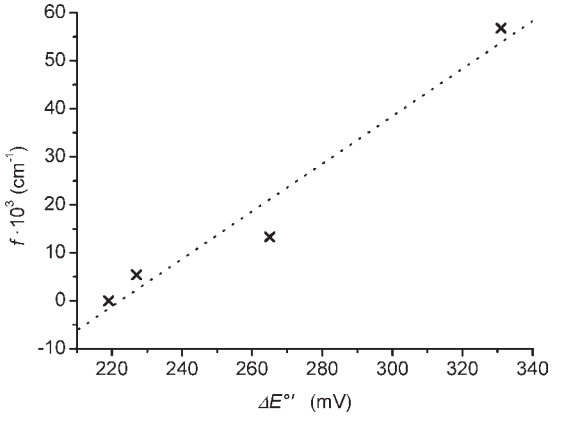

Figure 9. Correlation of the oscillator strength f of the IVCT absorptions and the $\Delta E^{o\prime}$ values of **5a**−**d** determined by NIR and cyclic voltammetry, respectively.

has been validated by the solvatochromic behavior of the IVCT band (Figure 5).[20]

Deconvolution of the NIR bands of **3a**−**d**$^+$ was performed using three overlapping Gaussian shaped absorptions. The sum of those Gaussian functions closely matches with the measured spectra (Figure 6, Supporting Information, Figures SI4 and SI5). This procedure allowed the determination of the extinctions and maxima of the IVCT bands. The ε_{max}, $\Delta\nu_{1/2}$, and ν_{max} values were reproducible within 25 L·mol^{-1}·cm^{-1}, 20 cm^{-1}, and 10 cm^{-1}, respectively. Thiophene **3a** exhibits an IVCT absorption at 5490 cm^{-1} with ε_{max} = 821 L·mol^{-1}·cm^{-1} ($\Delta\nu_{1/2}$ = 2519 cm^{-1}) being the lowest extinction within the series **3a**−**d**. However, the extinction increases from **3a** to **3d** (**3b**, ε_{max} = 1496 L·mol^{-1}·cm^{-1}, ν_{max} = 5060 cm^{-1} ($\Delta\nu_{1/2}$ = 2364 cm^{-1}); **3c**, ε_{max} = 3145 L·mol^{-1}·cm^{-1}, ν_{max} = 4750 cm^{-1} ($\Delta\nu_{1/2}$ = 2314 cm^{-1}); **3d**, ε_{max} = 4200 L·mol^{-1}·cm^{-1}, ν_{max} = 4820 cm^{-1} ($\Delta\nu_{1/2}$ = 2369 cm^{-1})) (Table 4). This tendency supports the results which were observed in the voltammetric studies (see above). The extinction of the IVCT absorptions and therefore, the degree of intermetallic communication, increases from electron poor **3a** to the electron rich **3d**.

Table 2. Cyclic Voltammetric Data of 3a−d[a]

compound	$E_1^{o\prime}$ in mV (ΔE_p in mV)[b]	$E_2^{o\prime}$ in mV (ΔE_p in mV)[c]	$\Delta E^{o\prime}$ in mV	ref.
3a	−94 (65)	166 (65)	260	this work
3b	−152 (60)	138 (63)	290	this work
3c	−206 (65)	204 (65)	410	this work
3d	−238 (68)	212 (75)	450	11

[a] Potentials vs FcH/FcH$^+$, scan rate 100 mV·s^{-1} at a glassy-carbon electrode of 0.5 mmol·L^{-1} solutions of **3a**−**d** in dry dichloromethane containing 0.1 mol·L^{-1} of [N(^{n}Bu)$_4$][B(C$_6$F$_5$)$_4$] as supporting electrolyte at 25 °C. [b] $E_1^{o\prime}$ = Potential of the 1st oxidation. [c] $E_2^{o\prime}$ = Potential of the 2nd oxidation.

Recently, the electrochemical behavior of 3,4-diferrocenylmaleimide was reported showing electron transfer properties at a comparable level to **3a**−**d**.[21] While the thiophene **3a** and furan **3b** exhibit lower $\Delta E^{o\prime}$ values and a lower extinction of the IVCT absorption band than 3,4-diferrocenylmaleimide, the pyrroles **3c** and **3d** showed a stronger intermetallic communication between the ferrocenyl termini.

The strength of the IVCT absorptions is expressed by the oscillator strength f, which can be calculated from ε_{max} and $\Delta\nu_{1/2}$ (fwhm = Full Width at Half Maximum) assuming Gaussian shaped transitions (eq 2).[22]

$$f = 4.6 \times 10^{-9} \cdot \varepsilon_{max} \cdot \Delta\nu_{1/2} \quad (2)$$

Within the class II regime the electronic coupling parameter H_{ab} can be calculated according to Hush's two state model as shown in eq 3, where r_{ab} is the distance between the two redox active sites and ε_{max}, $\Delta\nu_{1/2}$, and ν_{max} can be obtained from the appropriate NIR spectroscopic measurements.[23,24] The free energy of resonance stabilization ΔG_r, as contribution of the free energy of comproportionation ΔG_c° (eq 5a) can be derived from H_{ab} using eq 4.[23] Four factors contribute to the magnitude of ΔG_c° (eq 5a): (i) a statistical contribution $^1/_2RT \ln {}^1/_4$, (ii) an electrostatic factor (ΔG_e) arising from the repulsion of the two similarly charged metal centers linked by the bridging ligand, (iii) a synergistic factor (ΔG_s) due to metal−ligand backbonding interactions, and (iv) the aforementioned resonance stabilization factor (ΔG_r).[23,24] Assuming that the electron transfer distances are similar or identical, all contribution factors except the resonance stabilization ΔG_r are constant (eq 5b).

$$H_{ab} = 2.06 \times 10^{-2} \frac{\sqrt{\nu_{max} \cdot \varepsilon_{max} \cdot \Delta\nu_{1/2}}}{r_{ab}} \quad (3)$$

$$-\Delta G_r = \frac{2H_{ab}^2}{\nu_{max}} \quad (4)$$

$$\Delta G_c^o = -\Delta E^{o\prime} \cdot F = \frac{1}{2} RT \ln \frac{1}{4} + \Delta G_e + \Delta G_s + \Delta G_r \quad (5a)$$

$$\text{const} = \frac{1}{2} RT \ln \frac{1}{4} + \Delta G_e + \Delta G_s \quad (5b)$$

Combining eqs 2−5 and subsequent conversion leads to a linear relationship between the oscillator strength f, as product of ε_{max} and $\Delta\nu_{1/2}$, and $\Delta E^{o\prime}$ defined as peak separation of the

dx.doi.org/10.1021/ic200926z |Inorg. Chem. 2011, 50, 10623–10632

Table 3. Cyclic Voltammetric Data of 5a−d[a]

compound	$E_1^{o\prime}$ in mV [b] (ΔE_p in mV)	$\Delta E_1^{o\prime}$ in mV [c]	$E_2^{o\prime}$ in mV [b] (ΔE_p in mV)	$\Delta E_2^{o\prime}$ in mV [c]	$E_3^{o\prime}$ in mV [b] (ΔE_p in mV)	$\Delta E_3^{o\prime}$ in mV [c]	$E_4^{o\prime}$ in mV [b] (ΔE_p in mV)	ref.
5a	−161 (62)	← 219 →	58 (64)	← 360 →	418 (64)	← 186 →	604 (60)	9
5b	−237 (60)	← 227 →	−10 (60)	← 380 →	370 (62)	← 220 →	590 (61)	this work
5c	−280 (67)	← 265 →	−15 (68)	← 400 →	385 (71)	← 224 →	609 (72)	this work
5d	−280 (62)	← 331 →	51 (63)	← 272 →	323 (62)	← 227 →	550 (61)	11

[a] Potentials vs FcH/FcH^+, scan rate 100 mV·s^{-1} at a glassy-carbon electrode of 0.5 mmol·L^{-1} solutions of **5a−d** in dry dichloromethane containing 0.1 mol·L^{-1} of $[N(^nBu)_4][B(C_6F_5)_4]$ as supporting electrolyte at 25 °C. [b] $E_1^{o\prime}$ = potential of the 1st oxidation; $E_2^{o\prime}$ = potential of the 2nd oxidation; $E_3^{o\prime}$ = potential of the 3rd oxidation; $E_4^{o\prime}$ = potential of the 4th oxidation. [c] $\Delta E_1^{o\prime}$ = difference between 1st and 2nd redox potential; $\Delta E_2^{o\prime}$ = difference between 2nd and 3rd redox potential; $\Delta E_3^{o\prime}$ = difference between 3rd and 4th redox potential.

Table 4. NIR Data of the 2,5-Di- and 2,3,4,5-Tetraferrocenyl Heterocycles 3a−d and 5b−d [a]

compound	transition	ν_{max} (cm^{-1}) (ε_{max} (L mol^{-1} cm^{-1}))	$\Delta\nu_{1/2}$ (cm^{-1})
3a$^+$	IVCT	5490 (821)	2519
	LMCT	3643 (732)	1328
3b$^+$	IVCT	5060 (1496)	2364
	LMCT	3673 (2000)	1104
3c$^+$	IVCT	4750 (3145)	2314
	LMCT	4227 (1023)	958
3d$^+$	IVCT	4820 (4200)[b]	2369[b]
	LMCT	4256 (1805)	690
5b$^+$	IVCT	5631 (466)	2526
	LMCT	3445 (637)	1071
5b^{2+}	IVCT	6166 (449)	2606
	LMCT	3789 (261)	1078
5c$^+$	IVCT	6214 (1045)	2592
	LMCT	3826 (538)	1044
5c^{2+}	IVCT	6237 (948)	2682
	LMCT	4004 (564)	738
5d$^+$	IVCT	4752 (4900)[b]	2719[b]
	LMCT	3443 (2823)	1480

[a] In dry dichloromethane containing 0.1 mol·L^{-1} of $[N(^nBu)_4][B(C_6F_5)_4]$ as supporting electrolyte at 25 °C. [b] Ref 11.

oxidation events (electrochemical experiments, see above) (eq 6).

$$\frac{f}{4.6\times10^{-9}} = \varepsilon_{max}\Delta\nu_{1/2} = \frac{\text{const}\cdot r_{ab}^2}{8.49\times10^{-4}} + \frac{F\cdot r_{ab}^2}{8.49\times10^{-4}}\cdot\Delta E^{o\prime} \qquad (6)$$

Within these studies we were able to substantiate the preceding model by experimental data for the first time within one family of molecules. A linear relationship between the oscillator strength and $\Delta E^{o\prime}$ with a correlation coefficient of $R^2 = 0.980$ was observed (Figure 7). This verifies the examined 2,5-diferrocenyl heterocycles **3a−d** as class II systems (see above) revealing similar geometries and hence, similar electrostatic repulsions.

It is also possible to consecutively oxidize the ferrocenyls in supercrowded **5a−d** generating cations **5a−d**$^+$, **5a−d**$^{2+}$, **5a−d**$^{3+}$, and **5a−d**$^{4+}$, respectively, in dichloromethane and in presence of $[N^nBu_4][B(C_6F_5)_4]$ (0.1 mol·L^{-1}) as supporting electrolyte, as four ferrocenyl-related oxidation half reactions in the anodic CV sweep and reduction half reactions in the cathodic CV sweep are observed. Each of the four ferrocenyl entities showed a reversible electrochemical behavior with $60 \le \Delta E_p \le 72$ mV. Theoretically, electrochemical reversibility is characterized by ΔE_p values of 59 mV at 25 °C.[25] The data of the cyclic voltammetric studies are summarized in Table 3. It seems reasonable that the first two oxidations are mainly located at the ferrocenyl moieties in 2,5-position while further oxidation leads to ferrocenium ions in 3 and 4 position.[26] The potentials of the first redox process decrease in the series of **5a** (−161 mV), **5b** (−237 mV), and **5c** (−280 mV) as well as **5d** (−280 mV). The $\Delta E^{o\prime}$ values between the first and the second redox event follow the same trend as observed in the 2,5-diferrocenyl heterocycles **3a−d**, which correlates with the communication tendency of the iron centers. In consequence of the high steric demand of the ferrocenyl groups in **5a−d** the ferrocenyls are not coplanar with the heterocyclic core as evidenced from solid state structure (Figure 2), the $\Delta E_1^{o\prime}$ values are as expected smaller, when compared to the diferrocenyl analogues **3a−d**. The $\Delta E^{o\prime}$ values between the second and third redox process are additionally influenced by the different chemical environment of the ferrocenyls either to be in 2,5- or in 3,4-positions. Therefore, $\Delta E_2^{o\prime}$ does not necessarily correspond to the communication behavior of molecules **5a−d** and hence, these values are less expressive. The differences between the third and the fourth redox couples are, except for thiophene **5a** (186 mV), similar (220−227 mV), as the **5a−d**$^{3+}$ species show no communication (see UV−vis/NIR spectroscopic investigations, see below). The separation of these redox events are mostly attributed to electrostatic effects. Comparing the $\Delta E_1^{o\prime}$ values (Table 3) with the τ parameter obtained from single crystal X-ray data of **5a**, **5c**, and **5d** (Table 1) it can be recognized that the most delocalized species (highest τ value) also show the highest $\Delta E_1^{o\prime}$ value. This comparison would enable the possibility of predicting the electrochemical properties by single crystal X-ray diffraction analysis.

The spectro-electrochemical experiments carried out with **5a−d** were performed under similar conditions as in the studies of **3a−d** (see above). UV−vis/NIR spectra were recorded every 25, 50, or 100 mV in a potential range between −500 and 1500 mV vs Ag/Ag^+. During this procedure the neutral compounds **5a−d** were stepwise oxidized generating cations **5a−d**$^+$ (in the potential range of 200−350 mV), **5a−d**$^{2+}$ (450−550 mV), **5a−d**$^{3+}$ (750−900 mV), and **5a−d**$^{4+}$ (above 1000 mV). (see Supporting Information, Figures SI10−SI12 and refs 9,11) As outlined earlier the 2,3,4,5-tetraferrocenyl thiophene **5a** does not show any absorptions between 900−3000 nm; thus, no IVCT absorption could be detected in any oxidation state.[9]

dx.doi.org/10.1021/ic200926z |Inorg. Chem. 2011, 50, 10623–10632

However, **5d** shows strong IVCT absorptions (ε_{max} = 4900 $L \cdot mol^{-1} \cdot cm^{-1}$),[11] in the monocationic oxidation state while **5b** and **5c** exhibit much weaker bands in this region (**5b**$^+$, ε_{max} = 466 $L \cdot mol^{-1} \cdot cm^{-1}$; **5c**$^+$, ε_{max} = 1045 $L \cdot mol^{-1} \cdot cm^{-1}$). Upon potential increase to 500 mV a second oxidation occurs, and **5b**$^{2+}$ and **5c**$^{2+}$ are formed, whereby the IVCT absorptions were shifted hypsochromically (**5b**$^{2+}$, from ν_{max} = 5631 to 6166 cm^{-1}; **5c**$^{2+}$, from ν_{max} = 6214 to 6237 cm^{-1}) (Table 4) with slightly decreasing extinctions. Increasing the potential to 800 mV resulted in the decrease and disappearance of the IVCT absorptions in both complexes **5b** and **5c**, respectively.

The IVCT transitions observed in monocationic **5a**−**d**$^+$ show a correlation (R^2 = 0.960) with the $E_1^{\circ\prime}$ values determined by electrochemical studies similar to that observed for the 2,5-diferrocenyl heterocycles **3a**−**d** (please note that the statistical contribution in eq 5 changes form $^1/_2RT \ln {}^1/_4$ to $^1/_4RT \ln {}^1/_4$ in tetrametallic species) demonstrating, with exception of **5a** (see above), that they can be classified as class II systems. In summary, the communication between the corresponding ferrocenyl units in 2,3,4,5-tetraferrocenyl heterocycles **5a**−**c** is much lower than the one observed in the appropriate 2,5-diferrocenyl derivatives **3a**−**c**. This might be attributed to the higher steric demand in supercrowded **5a**−**c** and therefore the decreased possibility of the ferrocenyl units being coplanar with the central ^cC_4E core (E = S, O, N). The IVCT absorptions in the more electron rich systems (**3d**, **5d**) are more intense than those in the less electron rich ones (**3a**, **5b**). For **5a** no IVCT absorptions could be detected[9] which differs from all other heterocyclic compounds of this series. This behavior may be caused by (i) the electron poor character of the thiophene moiety versus the pyrrole unit, and (ii) the high steric demand of **5a** resulting in no observable interactions of the ferrocenyl moieties through the ^cC_4S core. The tendency of electron communication between the iron centers via the appropriate ^cC_4E connectivities in all newly prepared heterocyclic compounds depends on the electronic and steric properties of the respective species and in addition, on the delocalization which could be expressed as τ parameter derived from X-ray measurements (Table 1).

The correlation between the oscillator strength and the $\Delta E^{\circ\prime}$ values offer the possibility to calculate the effective electron transfer distance r_{ab} from the slope (m) of the least-squares line (eqs 6, 7 and Supporting Information).

$$r_{ab} = \sqrt{\frac{m \times 8.49 \times 10^{-4}}{F \times 4.6 \times 10^{-9}}} \qquad (7)$$

For molecules **3a**−**d** an r_{ab} value of 2.0 ± 0.1 Å is obtained, while for **5a**−**d** 3.35 ± 0.25 Å has been calculated. It seems reasonable that the crowded tetraferrocenyl species exhibit longer electron transfer distances compared to the diferrocenylated heterocycles, as a coplanarity of the ferrocenyl termini and the central ^cC_4E core (E = S, O, NMe, NPh) is less favorable and hence, electron delocalization from the ferrocenes to the heterocycle is hindered. Because of partial delocalization of the "redox orbital" into the heterocycle, r_{ab} is expected to be much shorter than the geometrical iron−iron distances.[27]

CONCLUSION

A series of 2,5-di- and 2,3,4,5-tetraferrocenyl heterocycles including thiophene, furan, and pyrrole could be synthesized using palladium-catalyzed Negishi *C,C* cross-coupling reactions. Single crystal X-ray diffraction analysis of selected compounds revealed differences in the electronic delocalization of the appropriate heterocyclic core system. For ease of comparison, we introduced τ as "degree" of delocalization, a normalized quotient of the single and double bond length, resulting in the observation that the heterocyclic core system in 2,3,4,5-tetraferrocenyl thiophene is much less delocalized compared to 2,3,4,5-tetraferrocenyl-1-methyl-1*H*-pyrrole and 2,3,4,5-tetraferrocenyl-1-phenyl-1*H*-pyrrole, respectively. Electrochemical studies such as cyclic voltammetry and square wave voltammetry were performed to investigate the redox behavior of the ferrocenyl-substituted heterocyclic compounds. We found that more electron-rich systems exhibit larger $\Delta E^{\circ\prime}$ values. This is attributed to a greater tendency of the iron centers to interact with each other in their mixed valence oxidation state. The metal−metal communication was further proven by NIR studies which revealed significant differences in the IVCT absorptions. All di- and tetraferrocenyl-functionalized molecules, except the 2,3,4,5-tetraferrocenyl thiophene, which is classified as class I, could be classified as class II systems according to Robin and Day.[28] These compounds show a linear relationship between the $\Delta E^{\circ\prime}$ values and the oscillator strength f of the IVCT transitions as predicted by theoretical hypothesis for a series of molecules with similar geometries and hence, similar electrostatic properties. This relation could be described for the first time in organometallic chemistry and offers the possibility to estimate r_{ab} which is notoriously difficult to obtain experimentally.

EXPERIMENTAL SECTION

General Conditions. All reactions were carried out under an atmosphere of nitrogen using standard Schlenk techniques. Tetrahydrofuran, toluene, *n*-hexane, and *n*-pentane were purified by distillation from sodium/benzophenone ketyl; dichloromethane was purified by distillation from calcium hydride.

Instruments. Infrared spectra were recorded with a FT-Nicolet IR 200 equipment. The ^{1}H NMR spectra were recorded with a Bruker Avance III 500 spectrometer operating at 500.303 MHz in the Fourier transform mode; the $^{13}C\{^1H\}$ NMR spectra were recorded at 125.800 MHz. Chemical shifts are reported in δ (parts per million) downfield from tetramethylsilane with the solvent as reference signal (^{1}H NMR: $CHCl_3$, δ 7.26; $^{13}C\{^1H\}$ NMR: $CDCl_3$, δ 77.00). The melting points of analytical pure samples (sealed off in nitrogen purged capillaries) were determined using a Gallenkamp MFB 595 010 M melting point apparatus. Microanalyses were performed using a Thermo FLASHEA 1112 Series instrument. Spectro-electrochemical measurements were carried out in an OTTLE cell similar to that described previously[29] from dichloromethane solutions containing 0.1 mol L^{-1} of $[N^nBu_4][B(C_6F_5)_4]$ as supporting electrolyte using a Varian Cary spectrometer. High resolution mass spectra were recorded using a micrOTOF QII Bruker Daltonite workstation.

Electrochemistry. Measurements on 0.5 or 1.0 $mmol \cdot L^{-1}$ solutions of the analytes in dry air free dichloromethane containing 0.1 $mol \cdot L^{-1}$ of $[N^nBu_4][B(C_6F_5)_4]$ as supporting electrolyte were conducted under a blanket of purified argon at 25 °C utilizing a Radiometer Voltalap PGZ 100 electrochemical workstation interfaced with a personal computer. A three electrode cell, which utilized a Pt auxiliary electrode, a glassy carbon working electrode (surface area 0.031 cm^2), and an Ag/Ag^+ (0.01 $mol \cdot L^{-1}$ $AgNO_3$) reference electrode mounted on a Luggin capillary was used. The working electrode was pretreated by polishing on a Buehler microcloth first with 1 μm and then 1/4 μm diamond paste. The reference electrode was constructed from a silver wire inserted into a solution of 0.01 $mol \cdot L^{-1}$ $AgNO_3$ and 0.1 $mol \cdot L^{-1}$

dx.doi.org/10.1021/ic200926z |*Inorg. Chem.* 2011, 50, 10623–10632

$[N^nBu_4][B(C_6F_5)_4]$ in acetonitrile, in a luggin capillary with a vycor tip. This luggin capillary was inserted into a second luggin capillary with vycor tip filled with a 0.1 mol·L^{-1} $[N^nBu_4][B(C_6F_5)_4]$ solution in acetonitrile. Successive experiments under the same experimental conditions showed that all formal reduction and oxidation potentials were reproducible within 5 mV. Experimentally potentials were referenced against an Ag/Ag^+ reference electrode, but results are presented referenced against ferrocene as an internal standard as required by IUPAC.[19] To achieve this, since the ferrocene couple FcH/FcH^+ interferes with the ferrocenyl signals of the analytes, each experiment was first performed in the absence of any internal standard, and then repeated in the presence of <1 mmol·L^{-1} decamethyl ferrocene (Fc*).[29] A separate experiment containing only ferrocene and decamethyl ferrocene was also performed. Data was then manipulated on a Microsoft Excel worksheet to set the formal reduction potentials of the FcH/FcH^+ couple to 0.0 V. Under our conditions the Fc^*/Fc^{*+} couple was at −619 mV vs FcH/FcH^+, ΔE_p = 60 mV, while the FcH/FcH^+ couple itself was at 220 mV vs Ag/Ag^+, ΔE_p = 61 mV.[30]

Single Crystal X-ray Diffraction Analysis. Single crystals of **3b** and **5c** suitable for X-ray diffraction analysis could be obtained by diffusion of *n*-hexane into a chloroform solution containing **3b** or **5c** at ambient temperature. Data were collected on an Oxford Gemini S diffractometer at 110 K using Mo−K_α (λ = 0.71073 Å) radiation. The structures were solved by direct methods and refined by full-matrix least-squares procedures on F^2.[31] All non-hydrogen atoms were refined anisotropically, and a riding model was employed in the treatment of the hydrogen atom positions.

CCDC 802797 (**3b**) and 802796 (**5c**) contain the supplementary crystallographic data for this paper. These data can be obtained free of charge from The Cambridge Crystallographic Data Centre via www.ccdc.cam.ac.uk/data_request/cif.

Reagents. 2,5-Diferrocenylthiophene,[8a] 2,5-dibromofuran,[32] 2,5-dibromo-1-methyl-1*H*-pyrrole,[14] 2,3,4,5-tetrabromo-1-methyl-1*H*-pyrrole,[14] 2,3,4,5-tetrabromofuran[15] and $[N^nBu_4][B(C_6F_5)_4]$[18] were prepared according to published procedures. All other chemicals were purchased from commercial suppliers and were used as received.

Gerneral Procedure−Synthesis of 2,5-Di- (3) and 2,3,4,5-Tetraferrocenyl Heterocycles (5). To 920 mg (5 mmol) of ferrocene and 56 mg (0.5 mmol) of KO*t*Bu dissolved in 20 mL of tetrahydrofuran, 4.6 mL (7.5 mmol) of a 1.6 M solution of *t*-butyllithium in *n*-pentane were added dropwise at −30 °C. After 1 h of stirring at this temperature, 2.2 g (8 mmol) of dry $[ZnCl_2 \cdot 2thf]$ were added in a single portion. The solution was kept for 1 h at −30 °C and an additional hour at 25 °C. Afterward, 35 mg (0.03 mmol) of $[Pd(PPh_3)_4]$ and 1.67 mmol of the appropriate 2,5-dibromoheterocycle (**1**) or 0.83 mmol of the respective 2,3,4,5-tetrabromoheterocycle (**4**) were added in a single portion, and the reaction solution was stirred for 48 h at 60 °C. After evaporation of all volatiles, the precipitate was dissolved in 200 mL of dichloromethane and washed three times with 100 mL portions of water. The organic phase was dried over $MgSO_4$, and the solvent was removed in oil-pump vacuum. The remaining solid was purified by column chromatography on alumina using a *n*-hexane-toluene mixture of ratio 1:1 (v/v) as eluent. All volatiles were removed under reduced pressure. The title compounds were obtained as orange solids.

Data for 2,5-Diferrocenylfuran 3b. Yield: 524 mg (1.20 mmol, 72% based on **1b**) Anal. Calcd for $C_{24}H_{20}Fe_2O$ (436.10): C, 66.10; H, 4.62; Found: C, 66.22; H, 4.59. Mp.: 238 °C. IR data (KBr): 3089 m, 2923 w, 1597 w, 1498 s,1417 s,1328 w, 1105 m, 1001 s, 819 s, 766 s.^{1}H NMR ($CDCl_3$, δ); 6.21 (s, 2H, C_4H_2O), 4.66 (pt, J_{HH} = 1.8 Hz, 4H, C_5H_4), 4.29 (pt, J_{HH} = 1.8 Hz, 4H, C_5H_4), 4.14 (s, 10 H, C_5H_5). ^{13}C $\{^1H\}$ NMR ($CDCl_3$, δ): 152.23 (C_4H_2O), 105.47 ($^iC-C_4H_2O$), 77.06 ($^iC-C_5H_4$), 69.52 (C_5H_5), 68.52 (C_5H_4), 65.34 (C_5H_4). HR-ESI-MS $[m/z]$: calcd for $C_{24}H_{20}Fe_2O$: 463.0213, found: 436.0231 $[M]^+$.

Crystal Data for 3b. $C_{24}H_{20}Fe_2O$, M = 436.10 g mol^{-1}, crystal dimensions 0.38 × 0.38 × 0.25 mm, T = 110 K, orthorhombic, *Pnma*, a = 8.21450(10), b = 22.6539(4), c = 9.8332(2) Å, V = 1829.86(5) Å^3, Z = 4, ρ_{calcd} = 1.583 g cm^{-3}, μ = 1.596 mm^{-1}, θ range = 3.23−26.00°, reflections collected: 16550, independent: 1829 (R_{int} = 0.0278), R_1 = 0.0206, wR_2 = 0.0531 $[I > 2\sigma(I)]$.

Data for 2,5-Diferrocenyl-1-methyl-1*H*-pyrrole 3c. Yield: 510 mg (1.14 mmol, 68% based on **1c**.) Anal. Calcd for $C_{25}H_{23}Fe_2N$ (449.15): C, 66.85; H, 5.16; N, 3.12; Found; C, 66.91; H, 5.18; N, 3.04. Mp.: 238 °C. IR data (KBr): 3089 m, 2923 w, 1597 w, 1498 s,1417 s,1328 w, 1105 m, 1001 s, 819 s, 766 s. ^{1}H NMR ($CDCl_3$, δ); 6.23 (s, 2H, C_4H_2N), 4.42 (pt, J_{HH} = 1.8 Hz, 4H, C_5H_4), 4.27 (pt, J_{HH} = 1.8 Hz, 4H, C_5H_4), 4.18 (s, 10 H, C_5H_5), 3.78 (s, 3H, CH_3). ^{13}C $\{^1H\}$ NMR ($CDCl_3$, δ): 131.31 (C_4H_2N), 108.29 ($^iC-C_4H_2N$), 80.08 ($^iC-C_5H_4$), 69.43 (C_5H_5), 68.28 (C_5H_4), 68.00 (C_5H_4), 33.05 (CH_3). HR-ESI-MS $[m/z]$: calcd for $C_{25}H_{23}Fe_2N$: 449.0524, found: 449.0490 $[M]^+$.

Data for 2,3,4,5-Tetraferrocenylfuran 5b. Yield: 400 mg (0.49 mmol, 60% based on **4b**.) Anal. Calcd for $C_{44}H_{36}Fe_4O$ (804.14): C, 65.75; H, 4.51; Found; C, 65.74; H, 4.54; Mp.: 188 °C. IR data (KBr): 3083 w, 2922 m, 2851 w, 1653 m, 1498 m, 1409 m, 1104 s, 1037 m, 1001 s, 817 vs, 736 m .^{1}H NMR ($CDCl_3$, δ); 4.83 (pt, J_{HH} = 1.8 Hz, 4H, C_5H_4), 4.43 (s, 10H, C_5H_5), 4.40 (pt, J_{HH} = 1.8 Hz, 4H, C_5H_4), 4.10 (pt, J_{HH} = 1.8 Hz, 4H, C_5H_4), 4.07 (pt, J_{HH} = 1.8 Hz, 4H, C_5H_4), 3.79 (s, 10H, C_5H_5). ^{13}C NMR (126 MHz, $CDCl_3$) δ 146.52 (C_4O), 121.02 (C_4O), 79.32 ($^iC-C_5H_4$), 78.66 ($^iC-C_5H_4$), 71.37(C_5H_4), 70.37 (C_5H_4), 69.49 (C_5H_5), 69.10 (C_5H_5), 68.37 (C_5H_4), 66.85 (C_5H_4). HR-ESI-MS $[m/z]$: calcd for $C_{44}H_{36}Fe_4O$: 804.0162, found: 804.0128 $[M]^+$.

Data for 2,3,4,5-Tetraferrocenyl-1-methyl-1*H*-pyrrole 5c. Yield: 393 mg (0.48 mmol, 58% based on **4c**). Anal. Calcd for $C_{45}H_{39}Fe_4N$ (817.18): C, 66.14; H, 4.81; N, 1.71; Found; C, 65.98; H, 5.01; N, 1.69. Mp.: 176 °C. IR data (KBr): 3083 w, 2922 m, 2851 w, 1653 m, 1498 m, 1409 m, 1104 s, 1037 m, 1001 s, 817 vs, 736 m. ^{1}H NMR ($CDCl_3$, δ); 4.76 (s, 3H, CH_3), 4.51 (pt, J_{HH} = 1.8 Hz, 4H, C_5H_4), 4.44 (pt, J_{HH} = 1.8 Hz, 4H, C_5H_4), 4.30 (s, 10H, C_5H_5), 4.03 (pt, J_{HH} = 1.8 Hz, 4H, C_5H_4), 3.96 (pt, J_{HH} = 1.8 Hz, 4H, C_5H_4), 3.74 (s, 10H, C_5H_5). ^{13}C NMR (126 MHz, $CDCl_3$) δ 127.17 (C_4N), 121.36 (C_4N), 84.94 ($^iC-C_5H_4$), 80.94 ($^iC-C_5H_4$), 72.58(C_5H_4), 71.50 (C_5H_4), 69.44 (C_5H_5), 68.93 (C_5H_5), 67.60 (C_5H_4), 66.11 (C_5H_4), 33.94 (CH_3). HR-ESI-MS $[m/z]$: calcd for $C_{45}H_{39}Fe_4N$: 817.0479, found: 817.0439 $[M]^+$.

Crystal Data for 5c. $C_{45}H_{36}Fe_4N \cdot 2CHCl_3$, M = 1052.88 g mol^{-1}, crystal dimensions 0.38 × 0.35 × 0.15 mm, T = 110 K, orthorhombic, *Aba*2, a = 17.6554(4), b = 41.9726(9), c = 11.4149(3) Å, V = 8458.9(3) Å^3, Z = 8, ρ_{calcd} = 1.654 g cm^{-3}, μ = 1.760 mm^{-1}, θ range = 3.23−26.00°, reflections collected: 17283, independent: 6842 (R_{int} = 0.0334), R_1 = 0.0313, wR_2 = 0.0743 $[I > 2\sigma(I)]$, absolute structure parameter: 0.020(13).[33]

■ ASSOCIATED CONTENT

Supporting Information. Figures giving further spectroscopic details and CIF files giving crystallographic data. This material is available free of charge via the Internet at http://pubs.acs.org. Crystallographic data for **3b** and **5c** are also available from the Cambridge Crystallographic Database as file nos. CCDC 802797 and 802796.

■ AUTHOR INFORMATION

Corresponding Author

*E-mail: heinrich.lang@chemie.tu-chemnitz.de. Phone: +49 (0)371-531-21210. Fax: +49 (0)371-531-21219.

■ ACKNOWLEDGMENT

We are grateful to the Fonds der Chemischen Industrie for generous financial support. D.S. thanks the Fonds der Chemischen Industrie for a fellowship.

■ REFERENCES

(1) (a) Klein, A.; Lavastre, O.; Fiedler, J. *Organometallics* **2006**, *25*, 635–643. (b) Fox, M. A.; Farmer, J. D.; Roberts, R. L.; Humphrey, M. G.; Low, P. J. *Organometallics* **2009**, *28*, 5266–5269. (c) Fox, M. A.; Roberts, R. L.; Baines, T. E.; Le Guennic, B.; Halet, J.-F.; Hartl, F.; Yufit, D. S.; Albesa-Jové, D.; Howard, J. A. K.; Low, P. J. *J. Am. Chem. Soc.* **2008**, *130*, 3566–3578. (d) Packheiser, R.; Ecorchard, P.; Rüffer, T.; Lohan, M.; Bräuer, B.; Justaud, F.; Lapinte, C.; Lang, H. *Organometallics* **2008**, *27*, 3444–3457. (e) Lohan, M.; Ecorchard, P.; Rüffer, T.; Justaud, F.; Lapinte, C.; Lang., H. *Organometallics* **2009**, *28*, 1878–1890. (f) Kowalski, K.; Winter, R. F. *J. Organomet. Chem.* **2009**, *694*, 1041–1048. (g) Santi, S.; Orian, L.; Durante, C.; Bencze, E. Z.; Bisello, A.; Donoli, A.; Ceccon, A.; Benetollo, F.; Crociani, L. *Chem.—Eur. J.* **2007**, *13*, 7933–7947.

(2) (a) Creutz, C.; Taube, H. *J. Am. Chem. Soc.* **1969**, *91*, 3988–3989. (b) Creutz, C.; Taube, H. *J. Am. Chem. Soc.* **1973**, *95*, 1086–1094. (c) D'Alessandro, D. M.; Dinolfo, P. H.; Davies, M. S.; Hupp, J. T.; Keene, F. R. *Inorg. Chem.* **2006**, *45*, 3261–3274. (d) D'Alessandro, D. M.; Keene, F. R. *Chem. Rev.* **2006**, *106*, 2270–2298. (e) Kaim, W.; Sarkar, B. *Coord. Chem. Rev.* **2007**, *251*, 584–594. (f) Ghumaan, S.; Sarkar, B.; Maji, S.; Puranik, V. G.; Fiedler, J.; Urbanos, F. A.; Jimenez-Aparicio, R.; Kaim, W.; Lahiri, G. K. *Chem.—Eur. J.* **2008**, *14*, 10816–10828. (g) Baitalik, S.; Dutta, S.; Biswas, P.; Flörke, U.; Bothe, E.; Nag, K. *Eur. J. Inorg. Chem.* **2010**, 570–588.

(3) (a) Zhou, G.; Baumgarten, M.; Müllen, K. *J. Am. Chem. Soc.* **2007**, *129*, 12211–12221. (b) Coropceanu, V.; Gruhn, N. E.; Barlow, S.; Lambert, C.; Durivage, J. C.; Bill, T. G.; Nöll, G.; Marder, S. R.; Brédas, J.-L. *J. Am. Chem. Soc.* **2004**, *126*, 2727–2731. (c) Nelsen, S. F. *Chem.—Eur. J.* **2000**, *6*, 581–588. (d) Heckmann, A.; Lambert, C.; Goebel, M.; Wortmann, R. *Angew. Chem., Int. Ed.* **2004**, *43*, 5851–5856. (e) Nelsen, S. F.; Ismagilov, R. F.; Powell, D. R. *J. Am. Chem. Soc.* **1996**, *118*, 6313–6314. (f) Nelsen, S. F.; Ismagilov, R. F.; Powell, D. R. *J. Am. Chem. Soc.* **1997**, *119*, 10213–10222. (g) Nelsen, S. F.; Ismagilov, R. F.; Powell, D. R. *J. Am. Chem. Soc.* **1998**, *120*, 1924–1925. (h) Nelsen, S. F.; Ismagilov, R. F.; Gentile, K. E.; Powell, D. R. *J. Am. Chem. Soc.* **1999**, *121*, 7108–7114. (i) Nelsen, S. F.; Trieber, D. A., II; Ismagilov, R. F.; Teki, Y. *J. Am. Chem. Soc.* **2001**, *123*, 5684–5694.

(4) (a) Jones, S. C.; Barlow, S.; ÓHare, D. *Chem.—Eur. J.* **2005**, *11*, 4473–4481. (b) Barlow, S.; O'Hare, D. *Chem. Rev.* **1997**, *97*, 637–669. (c) Bruce, I. M. *Coord. Chem. Rev.* **1997**, *166*, 91.(d) Ratner, M.; Jortner, J. *Molecular Electronics*; Blackwell Science: Malden, MA, 1997; (e) Tour, M. J. *Acc. Chem. Res.* **2000**, *33*, 791–804. (f) Collier, P. C.; Wong, W. E.; Belohradsky, M.; Raymo, M. F.; Stoddart, F. J.; Kuekes, J. P.; Williams, S. R.; Heath, R. J. *Science* **1999**, *285*, 391–394. (g) Carroll, R. L.; Gorman, Ch. B. *Angew. Chem., Int. Ed.* **2002**, *41*, 4378–4400. (h) Robertson, N.; McGowan, C. A. *Chem. Soc. Rev.* **2003**, *32*, 96–103.

(5) (a) Yu, Y.; Bond, A. D.; Leonard, P. W.; Lorenz, U. J.; Timofeeva, T. V.; Vollhardt, K. P. C.; Whitener, G. D.; Yakovenko, A. A. *Chem. Commun.* **2006**, 2572–2574. (b) Diallo, A. K.; Daran, J.-C.; Varret, F.; Ruiz, J.; Astruc, D. *Angew. Chem., Int. Ed.* **2009**, *48*, 3141–3145. (c) Lapinte, C. *J. Organomet. Chem.* **2008**, *693*, 793–801.

(6) (a) For example: Low, P. J.; Brown, N. J. *J. Clust. Sci.* **2010**, *21*, 235–278. (b) Jakob, A.; Ecorchard, P.; Linseis, M.; Winter, R. F.; Lang, H. *J. Organomet. Chem.* **2009**, *694*, 655–666. (c) Hamon, P.; Justaud, F.; Cador, O.; Hapiot, P.; Rigaut, S.; Toupet, L.; Ouahab, L.; Stueger, H.; Hamon, J.-R.; Lapinte, C. *J. Am. Chem. Soc.* **2008**, *130*, 17372–17383. (d) Delgado-Pena, F.; Talham, D. R.; Cowan, D. O. *J. Organomet. Chem.* **1983**, *253*, C43–C46. (e) Auger, A.; Muller, A. J.; Swarts, J. C. *Dalton Trans* **2007**, 3623–3633. (f) Donoli, A.; Bisello, A.; Cardena, R.; Benetollo, F.; Ceccon, A.; Santi, S. *Organometallics* **2011**, *30*, 1116–1121. (g) Brown, N. J.; Lancashire, H. N.; Fox, M. A.; Collison, D.; Edge, R.; Yufit, D. S.; Howard, J. A. K.; Whiteley, M. W.; Low, P. J. *Organometallics* **2011**, *30*, 884–894.

(7) (a) Levanda, C.; Bechgaard, K.; Cowan, D. O. *J. Org. Chem.* **1976**, *41*, 2700–2704. (b) Bruce, M. I.; Costuas, K.; Davin, T.; Ellis, B. G.; Halet, J.-F.; Lapinte, C.; Low, P. J.; Smith, M. E.; Skelton, B. W.; Toupet, L.; White, A. H. *Organometallics* **2005**, *24*, 3864–3881. (c) Coat, F.; Paul, F.; Lapinte, C.; Toupet, L.; Costuas, K.; Halet, J.-F. *J. Organomet. Chem.* **2003**, *683*, 368–378. (d) Coat, F.; Guillemot, M.; Paul, F.; Lapinte, C. *J. Organomet. Chem.* **1999**, *578*, 76–84. (e) Ghazala, S. I.; Paul, F.; Toupet, L.; Roisnel, T.; Hapiot, P.; Lapinte, C. *J. Am. Chem. Soc.* **2006**, *128*, 2463–2476. (f) Ding, F.; Wang, H.; Wu, Q.; Van Voorhis, T.; Chen, S.; Konopelski, J. P. *J. Phys. Chem. A* **2010**, *114*, 6039–6046.

(8) (a) Iyoda, M.; Kondo, T.; Okabe, T.; Matsuyama, H.; Sasaki, S.; Kuwatani, Y. *Chem. Lett.* **1997**, 35–36. (b) Wang, M. C. P.; Li, Y.; Merbouh, N.; Yu., H.-Z. *Electrochim. Acta* **2008**, *53*, 7720–7725. (c) Patoux, C.; Coudret, C.; Launay, J.-P.; Joachim, C.; Gourdon, A. *Inorg. Chem.* **1997**, *36*, 5037–5049.

(9) Hildebrandt, A.; Rüffer, T.; Erasmus, E.; Swarts, J. C.; Lang, H. *Organometallics* **2010**, *29*, 4900–4905.

(10) Hildebrandt, A.; Schaarschmidt, D.; van As, L.; Swarts, J. C.; Lang, H. *Inorg. Chim. Acta* **2011**, *374*, 122–118.

(11) Hildebrandt, A.; Schaarschmidt, D.; Lang, H. *Organometallics* **2011**, *30*, 556–563.

(12) Sanders, R.; Mueller-Westerhoff., U. T. *J. Organomet. Chem.* **1996**, *512*, 219–224.

(13) Ertas, E.; Ozturk, T. *Tetrahedron Lett.* **2004**, *45*, 3405–3407.

(14) Gilow, H. M.; Burton, D. E. *J. Org. Chem.* **1981**, *46*, 2221–2225.

(15) Hill, H. B.; Sanger, C. R. *Justus Liebigs Ann. Chem.* **1886**, *232*, 42–102.

(16) Smith, M. B.; March, J. *March's Advanced Organic Chemistry: Reactions, Mechanisms, and Structure*, 5th ed.; Wiley-VCH: New York, 2001; pp 20−36.

(17) Bird, C. W. ; Cheeseman, G. W. H. *Comprehensive Heterocycles*; Katritzky, A. R., Rees, C. W., Eds.; Pergamon Press: Oxford, 1984; Vol. 4, pp 1−10.

(18) For information concerning the use of $[N^nBu_4][B(C_6F_5)_4]$ as supporting electrolyte see: (a) LeSuer, R. J.; Buttolph, C.; Geiger, W. E. *Anal. Chem.* **2004**, *76*, 6395–6401. (b) Barrière, F.; Geiger., W. E. *J. Am. Chem. Soc.* **2006**, *128*, 3980–3989. (c) Gericke, H. J.; Barnard, N. I.; Erasmus, E.; Swarts, J. C.; Cook, M. J.; Aquino, M. A. S. *Inorg. Chim. Acta* **2010**, *363*, 2222–2232. (d) Fourie, E.; Swarts, J. C.; Lorcy, D.; Bellec, N. *Inorg. Chem.* **2010**, *49*, 952–959. (e) Swarts, J. C.; Nafady, A.; Roudebush, J. H.; Trupia, S.; Geiger, W. E. *Inorg. Chem.* **2009**, *48*, 2156–2165. (f) Chong, D.; Slote, J.; Geiger, W. E. *J. Electroanal. Chem.* **2009**, *630*, 28–34. (g) Nemykin, V. N.; Rohde, G. T.; Barrett, C. D.; Hadt, R. G.; Sabin, J. R.; Reina, G.; Galloni, P.; Floris, B. *Inorg. Chem.* **2010**, *49*, 7497–7509. (h) Nemykin, V. N.; Rohde, G. T.; Barrett, C. D.; Hadt, R. G.; Bizzarri, C.; Galloni, P.; Floris, B.; Nowik, I.; Herber, R. H.; Marrani, A. G.; Zanoni, R.; Loim, N. M. *J. Am. Chem. Soc.* **2009**, *131*, 14969–14978.

(19) Gritzner, G.; Kuta, J. *Pure Appl. Chem.* **1984**, *56*, 461–466.

(20) (a) Lohan, M.; Justaud, F.; Roisnel, T.; Ecorchard, P.; Lang, H.; Lapinte, C. *Organometallics* **2010**, *29*, 4804–4817. (b) Ziegler, M.; von Zelewsky, A. *Coord. Chem. Rev.* **1998**, *177*, 257–300. (c) Strautmann, J. B. H.; DeBeer George, S.; Bothe, E.; Bill, E.; Weyhermüller, T.; Stammler, A.; Bögge, H.; Glaser, T. *Inorg. Chem.* **2008**, *47*, 6804–6824. (d) Flood, A. H.; McAdam, C. J.; Gordon, K. C.; Kjaergaard, H. G.; Manning, A. M.; Robinson, B. H.; Simpson, J. *Polyhedron* **2007**, *26*, 448–455.

(21) Solntsev, V. P.; Dudkin, S. V.; Sabin, J. R.; Nemykin, V. N. *Organometallics* **2011**, *30*, 3037–3046.

(22) Zhu, Y.; Wolf, M. O. *J. Am. Chem. Soc.* **2000**, *122*, 10121–10125.

(23) (a) D'Alessandro, D. M.; Keene, F. R. *Chem. Soc. Rev.* **2006**, *35*, 424–440. (b) Hush, N. S. *Prog. Inorg. Chem.* **1967**, *8*, 391–444. (c) Hush, N. S. *Electrochim. Acta* **1968**, *13*, 1005–1023. (d) Brunschwig, B. S.; Creutz, C.; Sutin, N. *Chem. Soc. Rev.* **2002**, *31*, 168–184.

(24) For the use the two state model in the calculation of electronic coupling, see for example: (a) ÒDAlessandro, D. M.; Topley, A. C.;

Davies, A. C.; Keene, F. R. *Chem.—Eur. J.* **2006**, *12*, 4873–4884. (b) Ghumaan, S.; Sarkar, B.; Maji, S.; Puranik, V. G.; Fiedler, J.; Urbanos, F. A.; Jimenez-Aparicio, R.; Kaim, W.; Lahiri, G. K. *Chem.—Eur. J.* **2008**, *14*, 10816–10828. (c) Tanaka, Y.; Ishisaka, T.; Inagaki, A.; Koike, T.; Lapinte, C.; Akita, M. *Chem.—Eur. J.* **2010**, *16*, 4762–4776. (d) Siebler, D.; Förster, C.; Gasi, T.; Heinze, K. *Chem. Commun.* **2010**, *46*, 4490–4492. (e) Brown, N. J.; Lancashire, H. N.; Fox, M. A.; Collison, D.; Edge, R.; Yufit, D. S.; Howard, J. A. K.; Whiteley, M. W.; Low, P. J. *Organometallics* **2011**, *30*, 884–894. (f) Ghazala, S. I.; Paul, F.; Toupet, L.; Roisnel, T.; Hapiot, P.; Lapinte, C. *J. Am. Chem. Soc.* **2006**, *128*, 2463–2476. (g) Aguirre-Etcheverry, P.; O'Hare, D. *Chem. Rev.* **2010**, *110*, 4839–4864.

(25) (a) Evans, D. H.; O'Connell, K. M.; Peterson, R. A.; Kelly, M. J. *J. Chem. Educ.* **1983**, *60*, 290–293. (b) Mobbott, G. A. *J. Chem. Educ.* **1983**, *60*, 697–701. (c) Kissinger, P. T.; Heineman, W. R. *J. Chem. Educ.* **1983**, *60*, 702–706. (d) Van Benshoten, J. J.; Lewis, J. Y.; Heineman, W. R. *J. Chem. Educ.* **1983**, *60*, 772–778.

(26) (a) Schröter, S.; Stock, C.; Bach, T. *Tetrahedron* **2005**, *61*, 2245–2267. (b) Jin, B.; Tao, F.; Liu, P. *J. Electroanal. Chem.* **2008**, *624*, 179–185.

(27) (a) Mücke, P.; Linseis, M.; Záliš, S.; Winter, R. F. *Inorg. Chim. Acta* **2011**, *374*, 36–50. (b) Bublitz, G. U.; Laidlaw, W. M.; Denning, R. G.; Boxer, S. G. *J. Am. Chem. Soc.* **1998**, *120*, 6068–6075. (c) Treynor, T. P.; Boxer, S. G. *J. Phys. Chem. A* **2004**, *108*, 1764–1778. (d) Dinolfo, P. H.; Lee, S. J.; Coropceanu, V.; Brédas, J.-L.; Hupp, J. T. *Inorg. Chem.* **2005**, *44*, 5789–5797. (e) Lancaster, K.; Odom, S. A.; Jones, S. C.; Thayumanavan, S.; Marder, S. R.; Brédas, J.-L.; Coropceanu, V.; Barlow, S. *J. Am. Chem. Soc.* **2009**, *131*, 1717–1723.

(28) Robin, M. B.; Day, P. *Adv. Inorg. Chem. Radiochem.* **1967**, *10*, 247–423.

(29) Krejčik, M.; Daněk, M.; Hartl, F. J. *J. Electroanal. Chem.* **1991**, *317*, 179–184.

(30) Ruiz, J.; Daniel, M.-C.; Astruc, D. *Can. J. Chem.* **2006**, *84*, 288–299.

(31) (a) Sheldrick, G. M. *Acta Crystallogr., Sect. A* **1990**, *46*, 467–473. (b) Sheldrick, G. M. *SHELXL-97, Program for Crystal Structure Refinement*; Universität Göttingen: Göttingen, Germany, 1997.

(32) Keegstraa, M. A.; Klompa, A. J. A.; Brandsmaa, L. *Synth. Commun.* **1990**, *20*, 3371–3374.

(33) Flack, H. D. *Acta Crystallogr., Sect. A* **1983**, *39*, 876–881.